PHYSICAL REVIEW B **83**, 144426 (2011)

Uniaxial magnetic anisotropy in $Co_{2.25}Fe_{0.75}O_2BO_3$ compared to $Co_3O_2BO_3$ and Fe_3O_2BO ludwigites

J. Bartolomé,[1] A. Arauzo,[2] N. V. Kazak,[3] N. B. Ivanova,[4,5] S. G. Ovchinnikov,[3,6] Yu. V. Knyazev,[4] and I. S. Lyubutin[7]

[1]*Instituto de Ciencia de Materiales de Aragón and Departamento de Física de la Materia Condensada, CSIC–Universidad de Zaragoza, 50009 Zaragoza, Spain*

[2]*Servicio de Instrumentación Científica–Área de Medidas Físicas, Universidad de Zaragoza, Pedro Cerbuna 12, 50009 Zaragoza, Spain*

[3]*L.V. Kirensky Institute of Physics, SB of RAS, 660036, Akademgorodok, Krasnoyarsk, Russia*

[4]*Siberian Federal University, 660074, Kirensky street 26, Krasnoyarsk, Russia*

[5]*Krasnoyarsk State Agrarian University, Mira street 90, Krasnoyarsk, Russia*

[6]*Siberian State Aerospace University, Krasnoyarskiy Rabochiy street 31, Krasnoyarsk, Russia*

[7]*Shubnikov Institute of Crystallography, RAS, 119333, Leninskiy prospect 59, Moscow, Russia*

(Received 14 December 2010; published 26 April 2011)

Magnetic and Mössbauer spectroscopy (MS) measurements have been performed on a single crystal of $Co_{2.25}Fe_{0.75}O_2BO_3$ with ludwigite structure. Two magnetic transitions ($T_N = 115$ K and $T_C = 70$ K) were traced from the ac susceptibility temperature dependence. The MS spectra as a function of temperature clearly show the onset of magnetic ordering below 115 K. Magnetization measurements on the parent $Co_3O_2BO_3$ and $Fe_3O_2BO_3$ compounds have been done for comparison. In $Fe_3O_2BO_3$ the anisotropy of the different phases has been determined, showing that the anisotropy axis changes from the *a* to the *b* axis in the low-temperature antiferromagnetic phase. High magnetic uniaxial anisotropy has been detected for both $Co_3O_2BO_3$ and $Co_{2.25}Fe_{0.75}O_2BO_3$. From the angle-dependent magnetization measurements it is found that in both compounds the easy axis of magnetization is the *b* [010] axis, where an antiferromagnetic component is superimposed on the main ferromagnetic component. In the *c* direction the behavior is purely antiferromagnetic. In $Co_{2.25}Fe_{0.75}O_2BO_3$ a strong reduction of the remanent magnetization and a very strong increase in coercive field along the *b* axis with respect to those found in $Co_3O_2BO_3$ were observed from magnetic hysteresis cycles measured below T_C. The increase of coercive field is caused by the increase of defects upon Co substitution by Fe.

DOI: 10.1103/PhysRevB.83.144426 PACS number(s): 75.50.Gg, 75.50.Vv, 75.30.Gw

I. INTRODUCTION

Homometallic and heterometallic oxyborates with one or several transition metal ions have been intensively investigated owing to their interesting magnetic and structural properties. These materials crystallize in several structures. Oxyborates with a ludwigite crystal structure (space group *Pbam*, $Z = 4$) are of the general formula $M_2M'(BO_3)O_2$ where *M* acts as a divalent ion and *M′* is trivalent. Both types of ion occupy the four nonequivalent crystallographic positions (Fig. 1). In Wyckoff notation these positions are 2*a*, 2*d*, 4*g*, and 4*h* and we number them as 1, 2, 3, and 4 correspondingly. The probability of occupation by a di- or trivalent ion is different for each position. The ludwigite crystal structure consists of low-dimensional subunits: two three-leg ladders (3LLs) of different types. The columns of edge-sharing octahedra form zigzag walls spreading along the crystallographic *c* axis. Mixed valence, complex distribution of magnetic ions among crystallographic positions, and strong electron correlations allow a variety of magnetic structures, charge ordering, and structural and electronic transitions to appear. The heterometallic compounds, where *M* and *M′* are ions of different sorts, have been so far the object of different studies.[1–4]

The ions in the 4-2-4 positions form so-called triads arranged as the rungs of a three-leg ladder of type I, which constitutes the main element of the ludwigite crystal structure. The distance between the transition ions in the sites 2 and 4 is the shortest and allows direct overlap of their electron orbitals. In addition, the ions in the 1 and 3 positions form a three-leg ladder of type II. [Note: we adhere to the notation given in Ref. 5 for the Fe sites and triads (see Fig. 1).]

These series have attracted much interest after the observation of a phase transition in $Fe_3O_2BO_3$ at $T_{CD} = 283$ K due to excitonic instability.[6,7] Short and long Fe-Fe bonds are formed in the 4-2-4 triads in the direction perpendicular to the axis of the ladder, with a doubling of the cell parameter on the *c* axis that affects the magnetic properties of the material. In this work the magnetic properties of the substitutional compound $Co_{2.25}Fe_{0.75}O_2BO_3$ are studied and compared to those of the parent compounds $Co_3O_2BO_3$ and $Fe_3O_2BO_3$—the two homometallic oxyborates with ludwigite structure available now.

At present there exist quite some experimental data for $Fe_3O_2BO_3$: x-ray diffraction,[5,6,8] neutron powder diffraction (NPD),[8,9] magnetic measurements,[6,10] Mössbauer spectroscopy (MS),[5,10–14] electron paramagnetic resonance,[15] and theoretical works.[7,16] The properties of this compound are summarized as follows:

(a) Four phase transitions in $Fe_3O_2BO_3$ with preferable occupation of nonequivalent crystallographic positions by Fe ions in varying valence states have been observed. Early MS experiments[5] have shown that the sites 1 and 3 are occupied by Fe^{2+} ions, while sites 2 and 4 were apparently occupied by Fe^{3+} ions. (1) It undergoes a structural transition at $T_{CD} = 283$ K, when being cooled, in the form of a subtle dimerization of iron ion pairs along 3LLs type I and charge localization,[6,11] while the Fe^{2+} (sites 1 and 3) play no role in this transition.[11] Above T_{CD} the ions in the sites 2 and 4 are occupied by Fe^{3+} cations with one additional electron per rung, while below T_{CD} mixed-valence ion pairs are formed.[11] The magnetic state is paramagnetic (PM). (2) At $T_{N1} = 112$ K, there is an antiferromagnetic transition (AFM1) where the Fe_2 and Fe_4 moments become ordered, and they

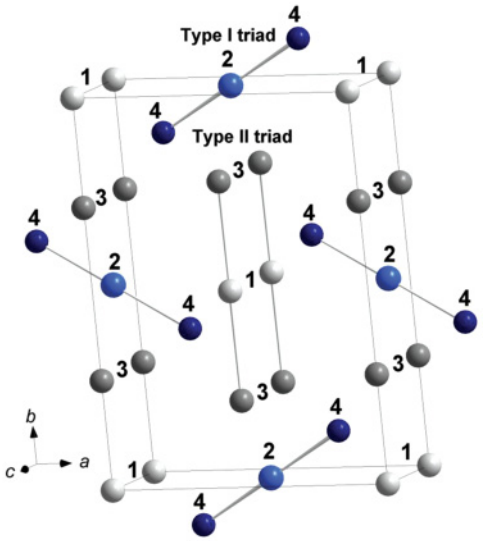

FIG. 1. (Color online) The crystal structure of $M_2M'O_2BO_3$ ludwigites. The nonequivalent crystallographic sites 1, 2, 3, and 4 are numbered. The transition metal ions in the sites 2 and 4 form triads of type I, and the ions in the sites 1 and 3 form triads of type II.

share one electron in a mixed-valence state. Otherwise, Fe_1 and Fe_3 sublattices are disordered, although Fe_3 is subject to a transferred weak hyperfine field from the already ordered Fe_2 and Fe_4 sublattices. (3) On further cooling, a new transition at $T_{N2} = 74$ K is observed where Fe_1 and Fe_3 also become ordered, and all other Fe moments reorient giving rise to a canted weak ferromagnetic (F) phase. Mixed-valence pairs in the Fe_4-Fe_2-Fe_4 rungs were clearly observed. (4) Below $T_{N3} = 50$ K there is charge order in the mixed-valent pair and the extra electron is localized at Fe_2.[10,11] The low-temperature phase was reported as antiferromagnetic (AFM2).[14] In all these results an electron hopping mechanism of the extra electron within the rung and between rungs is invoked to explain the different transitions.

(b) In a recent recent x-ray and NPD study[8] it is stated that (1) below T_{CD} the magnetic phase is paramagnetic. (2) Below $T_{N1} = 112$ K the high-temperature antiferromagnetic (AFM1) phase consists of Fe_4-Fe_2-Fe_4 AFM chains ferromagnetically coupled along the rungs of the 3LLs of type I, with the moments oriented in the b direction, and with practically identical moment value between the three Fe cations. In contrast, the Fe_1 and Fe_3 in 3LLs of type II support no magnetic moment. (3) Below $T_{N2} = 74$ K, (F) phase, the magnetic cell unit is doubled ($Z = 8$), the Fe_1 and Fe_3 belonging to 3LLs of type II develop a nonzero magnetic moment in the a direction, and order as ferromagnetic chains coupled antiferromagnetically along the c axis. It is reported that the Fe_1 and Fe_3 moments are different and opposed, giving rise to a net moment in the a direction of 2.36 μ_B/f.u. Thus, there are some conflicting results between the MS and NPD studies. Of course, MS is a local probe, while NPD is a bulk one, so some differences may be expected. Notwithstanding this fact, the differences are that (1) the WF phase is rather a ferrimagnetically ordered magnetic phase according to NPD and (2) the AFM2 phase is not observed in NPD.

In the case of the homometallic $Co_3O_2BO_3$, there is scarce information available, because high-quality and large enough crystals were obtained only recently.[17–20] At first, it seemed reasonable to assume the properties of $Co_3O_2BO_3$ to be analogous to those of $Fe_3O_2BO_3$. However, the extensive study of the structural, magnetic, and thermodynamic properties of $Co_3O_2BO_3$ showed that, in contrast,

(a) there is no structural transition in this compound;
(b) there is no partial magnetic ordering.

The investigations of $Co_3O_2BO_3$ are not completed up to now, and its magnetic structure is not precisely defined. However, a magnetic and thermodynamic study, carried out in Ref. 20, clearly showed only one magnetic transition near $T_N = 42$ K. Below this temperature the magnetic order is of ferrimagnetic or weak ferromagnetic type with an *ab* easy plane anisotropy.[18] The picture of magnetic ordering is much simpler for $Co_3O_2BO_3$ than for $Fe_3O_2BO_3$.

So, surprisingly, the structural and magnetic properties of $Fe_3O_2BO_3$ and $Co_3O_2BO_3$ appear to be quite different. This unexpected difference has led to renewed interest in the mixed Co-Fe ludwigites. In this paper, we have partially substituted Co by Fe ions and synthesized single-crystals of $Co_{3-x}Fe_xO_2BO_3$ to study their magnetic properties in comparison with the parent compounds. We reconsidered first the two pure compounds to determine their anisotropic behavior, so that a detailed comparison could be established. In Ref. 21, devoted to the mixed compound $Co_2FeO_2BO_3$, it was established that the magnetic properties of this ludwigite are close to those of $Fe_3O_2BO_3$ and not to $Co_3O_2BO_3$. However, for $x = 0.75$, there is no evidence of the structural transition which takes place in $Fe_3O_2BO_3$.

II. EXPERIMENTAL TECHNIQUES

Single crystals of $Co_{3-x}Fe_xO_2BO_3$ were grown by the flux method in the system Co_3O_4-Fe_2O_3-B_2O_3-PbO-PbF_2. The relative content of Co and Fe ions in the prepared compounds was first estimated from the mass ratio of the initial components, $Fe_2O_3/(Fe_2O_3 + Co_3O_4)$, and was later checked by X-ray and Mössbauer measurements. At relatively high Co:Fe ratio in the solution (>2.5) we have succeeded in preparing high-quality single crystals of $Co_{3-x}Fe_xO_2BO_3$ with ludwigite structure and maximal substitution (x value) near 1. All the samples were of needle shape up to 4 mm long. The maximal sample mass was about 1.2 mg. By lowering the Co:Fe concentration ratio in the solution a tendency to the synthesis of the warwickite phase appears in our synthetic process. At equal concentrations of cobalt and iron ions in the solution, single crystals of warwickite structure with lattice parameters $a = 3.134(2)$, $b = 9.269(7)$, and $c = 9.430(7)$ were grown.

The x-ray diffraction measurements were performed with a SMART APEX II diffractometer (Mo $K\alpha$ radiation, CCD detector). The scanning angle $2\theta = 5.4°$–$58°$ ($R1 = 1.40\%$, $wR2 = 3.31\%$).

The ^{57}Fe Mössbauer spectra were recorded at temperatures between 80 and 300 K in transmission geometry with a standard spectrometer operating in the constant acceleration regime. A nitrogen flow cryostat was used for the

low-temperature measurements. The γ-ray source ^{57}Co(Rh) was at room temperature, and the isomer shifts were measured relative to the metal α-Fe at room temperature. The number of channels used was 1024. The spectrometer linewidth with a standard α-Fe absorber and the NaI(Tl)- detector is <0.25/mm/s. The spectra were fitted with the UNIVEMMS program.

ac susceptibility measurements were performed in a superconducting quantum interference device (SQUID) magnetometer with ac option, in the frequency range $10 < f <$ 937 Hz, with an exciting field of 4 Oe. The angle-dependent magnetization $M(\theta_H, T)$ on oriented single crystals was measured with a rotating sample holder option in the SQUID magnetometer up to 50 kOe and with a vibrating sample magnetometer up to a bias field of 90 kOe. The temperature ranges are shown in Sec. IV.

The samples are highly anisotropic,[18] so they were oriented and placed in the sample holder along the desired axis with a four-circle x-ray diffractometer. They were positioned using vacuum grease and fixed with glue to prevent them from falling. For the sake of comparison with $Co_3O_2BO_3$ and $Fe_3O_2BO_3$, their magnetic properties which are not available in the literature, like hysteresis cycles of an oriented single crystal, were measured.

III. X-RAY DIFFRACTION AND MÖSSBAUER EFFECT

The crystallographic structures of the single crystals $Co_3O_2BO_3$ and $Co_{2.25}Fe_{0.75}O_2BO_3$ was solved in detail by means of single-crystal x-ray diffraction, and the results were given in Ref. 22. For both compounds the space group is *Pbam*. The lattice parameters of the parent compound $Co_3O_2BO_3$ are in good agreement with those published earlier.[20] For the solid solution ludwigite $Co_{2.25}Fe_{0.75}O_2BO_3$ the lattice parameters are $a = 9.282$, $b = 12.231$, and $c = 3.029$ Å. According to the x-ray diffraction data there is a pronounced preference in the occupation of distinct crystallographic sites by iron ions. Site 4 is the most preferable (similar data were obtained in Ref. 21 for $Co_2FeO_2BO_3$), with site 2 the next preferred.

The room temperature (RT) Mössbauer data of Ref. 22 have shown that iron enters into the ludwigite structure mostly in a trivalent state and nonuniformly distributed in the lattice. According to the RT MS, site 4 possesses the highest occupation factor for Fe ions (0.78), site 2 is the next (0.18), and for sites 1 and 3 the iron occupation factors are small (0.1 and <0.01, respectively). Thus, according to the investigations described in Ref. 21 and our previous work,[22] iron ions clearly prefer the positions inside the type-I triads.

In the present work we investigated the temperature evolution of the MS spectra in the temperature interval 80–300 K. The spectra were obtained for a powder of crushed $Co_{2.25}Fe_{0.75}O_2BO_3$ single crystals (see Fig. 2). The most evident feature is the pronounced temperature evolution upon cooling which begins near 110 K, where the splitting of quadrupole doublets into sextets by hyperfine interaction becomes observable. Remarkably, magnetic ordering in $Co_{2.25}Fe_{0.75}O_2BO_3$ appears near the same temperature as in $Fe_3O_2BO_3$, while $Co_3O_2BO_3$, much closer in cobalt content to our $Co_{2.25}Fe_{0.75}O_2BO_3$, does not show such a transition.

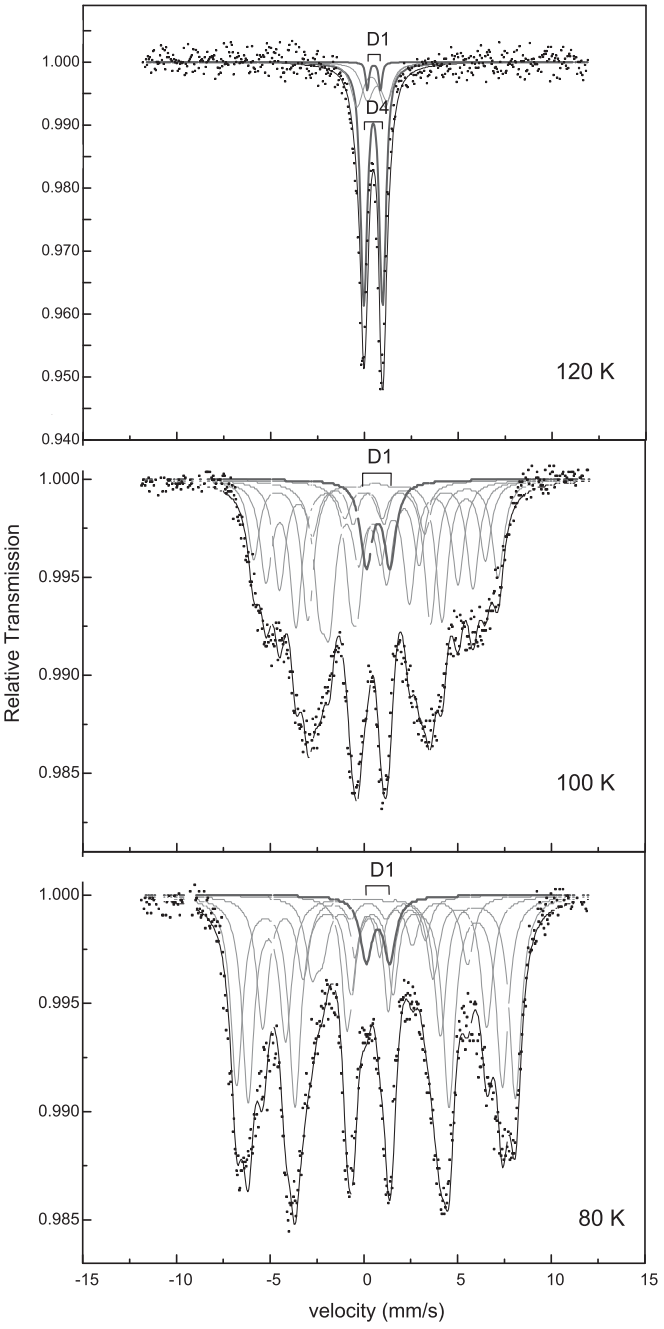

FIG. 2. Representative Mössbauer spectra of $Co_{2.25}Fe_{0.75}O_2BO_3$ at selected temperatures.

In analyzing the MS spectra we proceeded from the assumption that iron ions occupy a discrete set of crystallographic sites, as is previously shown in Refs. 21 and 22, but are not randomly distributed in the lattice. In the paramagnetic region at temperatures between 120 and 300 K, the MS spectra can be well described by four quadrupole doublets $D1$, $D2$, $D3$, and $D4$. As shown in Fig. 3, the isomer shift values δ for three doublets $D2$, $D3$, and $D4$ are in the range of 0.28–0.47 mm/s (at 130 K) which is typical of iron ions in the trivalent Fe^{3+} high-spin state. The isomer shift for doublet $D1$ is much higher ($\approx$0.85 mm/s) and its value is close to that for iron ions in the intermediate ($Fe^{2.5+}$–Fe^{2+}) valence state.

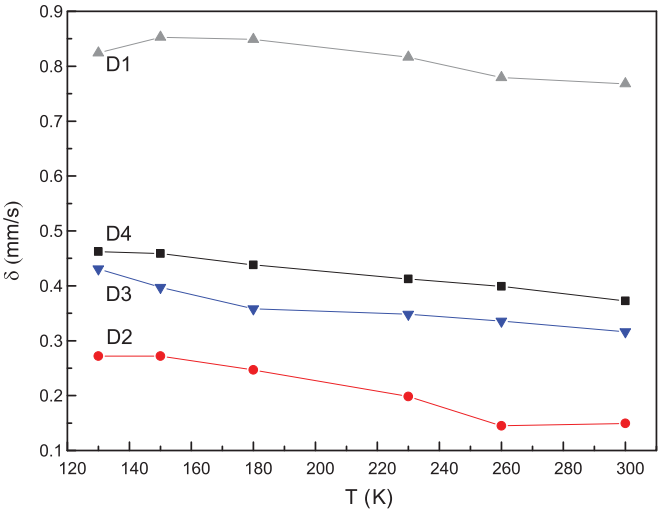

FIG. 3. (Color online) Temperature dependence of the isomer shift values obtained from the MS spectra for four quadrupole doublets (four nonequivalent iron sites) in the paramagnetic state of $Co_{2.25}Fe_{0.75}O_2BO_3$.

We found that the temperature dependences of the isomer shift values in the paramagnetic state (see Fig. 3) are close to those for $Fe_3O_2BO_3$,[13] and in general they follow the Doppler second-order (temperature) shift.

The doublet $D4$ clearly dominates in area, and it seems reasonable to assign it to the Fe^{3+} in site 4. Between 110 and 120 K magnetic splitting of the doublets begins and below 110 K the MS spectra may be described by four sextets and one low-area doublet with $\delta = 0.75$ mm/s and quadruple splitting $\Delta = 1.25$ mm/s. In the paramagnetic state this doublet belongs to the $D1$ component in Fig. 3.

The MS spectra of the parent $Fe_3O_2BO_3$ between 70 and 115 K have also been described by some sextets and one doublet.[13,14] The doublet was assigned to the Fe^{2+} ions in site 1, and it was supposed[14] that these ions are magnetically disordered in $Fe_3O_2BO_3$ down to $T = 70$ K. Fe^{2+} in site 3 was also considered as disordered, though a weak hyperfine field of transferred origin was observed. The Fe_2 and Fe_4 ions are magnetically ordered near $T = 110$ K.

Most probably, the doublet $D1$ in our sample also corresponds to the paramagnetic Fe^{2+} (or/and $Fe^{2.5+}$) ions, but due to the small doublet area (about 5% of the total iron area) its relative contribution to magnetic properties is negligible.

Below $T = 110$ K, the isomer shift and quadruple splitting values for the Fe^{3+} iron in the dominant site 4 are temperature independent ($\delta = 0.46$ mm/s, $\Delta = 1.0$ mm/s), while the magnetic hyperfine field at iron nuclei, B_{hf}, increases as the temperature decreases (Fig. 4).

Comparing our MS data for $Co_{2.25}Fe_{0.75}O_2BO_3$ with the same obtained for the parent compound $Fe_3O_2BO_3$,[13] one can conclude that the picture has a pronounced similarity in both cases, mainly consisting in the evidence of magnetic ordering near 110 K. Also in both considered ludwigites there is a fraction of the magnetic ions remaining disordered down to 70 K. Probably they are Fe^{2+} ions in crystallographic sites 1, but in our case of $Co_{2.25}Fe_{0.75}O_2BO_3$ their contribution is small.

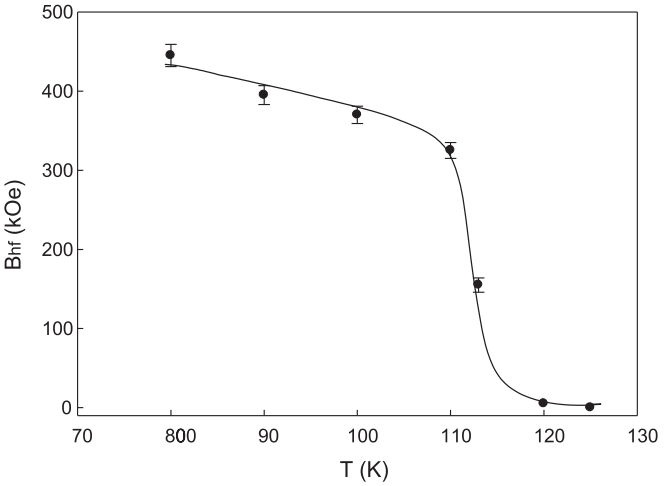

FIG. 4. The temperature dependence of the magnetic hyperfine field B_{hf} at iron ion nuclei at site 4 of $Co_{2.25}Fe_{0.75}O_2BO_3$. The solid line is a guide to the eye.

IV. MAGNETIC PROPERTIES

In this section the results obtained from rotating angle $M(\theta_H, T)$ and $M(H)$ measurements for the parent compounds $Co_3O_2BO_3$ and Fe_3O_2BO are presented first. This facilitates the understanding of $Co_{2.25}Fe_{0.75}O_2BO_3$ magnetic properties. It is known that in both Co and Fe pure compounds the c axis is a hard magnetization direction;[18] therefore only the anisotropy in the ab plane has been studied below.

A. $Co_3O_2BO_3$

This compound has just one magnetic phase transition to a ferromagnetic phase at $T_C = 42$ K.[20] In $M(\theta_H, T)$ measurements we could determine that the easy magnetization direction (EMD) in the ordered phase is the b axis (not shown). In Fig. 5 the hysteresis cycles for the compound $Co_3O_2BO_3$, measured below T_C on a single crystal along its b axis, are given. Although the remanent magnetization $M_r = 3.4(1)$ μ_B/f.u. remains practically constant, the coercive field H_c increases as

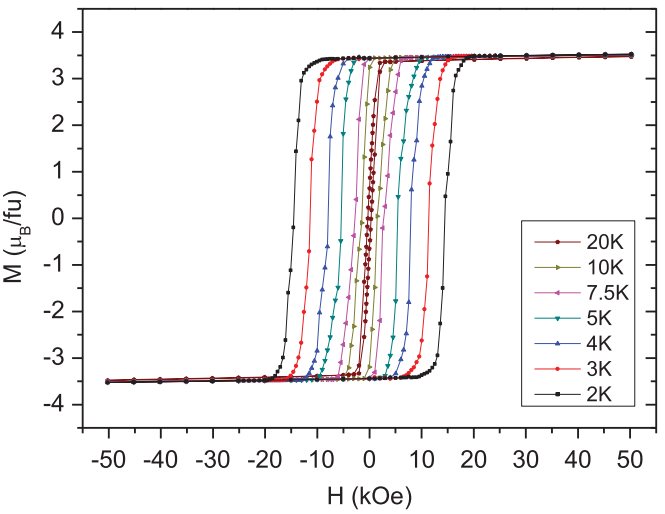

FIG. 5. (Color online) Hysteresis cycles of a $Co_3O_2BO_3$ sample as a function of $T (T < T_N)$. H parallel to b axis.

TABLE I. Collected magnetic transition temperature data for $Co_{3-x}Fe_xO_2BO_3$ from χ_{ac} or $M(T)$ (rows 1–3), easy magnetization direction at $T<T_C$ (row 4), and data extracted from high-T susceptibility (rows 5–8) and from hysteresis cycles (rows 9 and 10). The references to other work are indicated by superscripts. By the asterisk we mark the values calculated by us using the data presented in the corresponding reference. The present work results are shown in bold.

	x			
	0	0.75	1	3
T_{N3} (K)				40[10], **30.0(5)**
T_C (K), T_{N2} (K)	42[20]	**70.0(5)**	70[21]	70[10], **70.0(5)**
T_N (K), T_{N1} (K)		**115.0(5)**	117[17]	112[10], **110.7(5)**
EMD ($T<T_C$)	***b***	***b***	?	***a***
μ_{eff} /f.u. (μ_B)	7.20[20]	**7.28(2)**	7.53[21]	9.34*[6], **8.01**
μ_S/f.u. (μ_B)	**7.35**	**7.89**	**8.06**	**9.11**
μ_J/f.u. (μ_B)	**5.52**	**6.27**	**6.51**	**9.01**
θ_C (K)	−25[20]	**−69(3)**	−82[21]	−485[6], **−436**
M_r (μ_B/f.u.)	1.8*[20], **3.4(1)**	**0.9(1)**	0.48*[21]	2.36*[8], 0.1[10], **0.16**
χ_{AFM} (emu/mol)	**0.024(1)**	**0.029(3)**	0.036*[21]	**0.026**

the temperature is lowered. The small slope of $M(H)$ at high fields indicates the existence of a small superimposed antiferromagnetic susceptibility, with the value $\chi_{\text{AFM}} = 0.024(1)$ (emu/mol) (see Table I). Additionally, in the hysteresis cycles measured at fixed temperature $T = 2$ K, Fig. 6, the coercive field increases when the angle θ_H between the applied field and the b axis increases, following a $1/\cos\theta_H$ dependence.

B. $Fe_3O_2BO_3$

This compound is known to undergo a charge ordering transition at $T_{CD} = 283$ K, and three successive magnetic transitions as the temperature is lowered (PM-AFM1-F-AFM2). The transition temperatures we have measured are $T_{N1} = 110.7(5)$ K, $T_{N2} = 70.0(5)$ K, and $T_{N3} = 30.0(5)$ K, in reasonable agreement with previous findings.[10] It is convenient to remember in the discussion, as determined from NPD measurements,[8] that in all ordered phases the Fe_2 and Fe_4 sublattice magnetizations are parallel to the b axis, while only in the F phase do the Fe_1 and Fe_3 sublattice magnetizations bear a nonzero moment along the a axis. Although the AFM2 phase could not be discerned from NPD, MS gave evidence of this low-temperature phase when the angle θ between B_{hf} and V_{zz} (electric field gradient) for the different Fe sites became different from those in the AFM1 or F phase.[10,11,14]

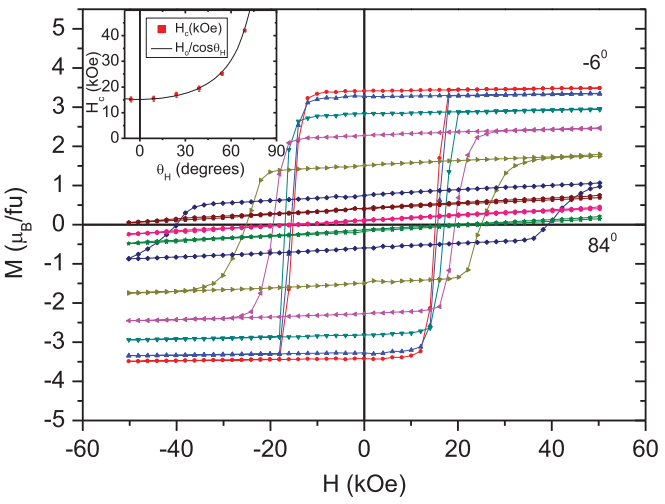

FIG. 6. (Color online) Hysteresis cycles of a $Co_3O_2BO_3$ single crystal at $T = 2$ K, as a function of rotation around the c axis. The extreme values of θ_H are indicated. The inset shows the variation of H_C as a function of θ_H. The fit to a $1/\cos\theta_H$ function is also shown.

Surprisingly, the detailed magnetization anisotropy directions of the different phases in this much studied compound have not been unambiguously determined up to date, since the measurements were performed on randomly oriented powders or small collections of crystals. To unravel this question the same methodology of rotating sample magnetometry around the c axis has been applied to a $Fe_3O_2BO_3$ single crystal. In Fig. 7, where the $M(\theta,T)$ data measured at 50 kOe are shown, it is evidenced that the antiferromagnetic phase AFM1 ($T_{N1} > T > T_{N2}$) is anisotropic, with the a axis as EMD at $H = 50$ kOe. Below T_{N2}, the ferromagnetic phase F is strongly anisotropic, with the a axis as the EMD. The observed magnetization reversal process is characteristic for a system of anisotropy field much higher than the coercive field (see below).

In Fig. 8 the hysteresis cycles measured along the a direction at different temperatures are depicted. As the compound is cooled from room temperature, at T_{N2} in the F phase the cycle opens, as expected for a ferrimagnetic phase. The coercive field increases with decreasing temperature and the remanence M_r decreases. At $T = 30$ K there is no coercivity and M_r becomes zero, as the system transforms into the AFM2 phase (see Fig. 8 inset). This temperature is 10 K lower than T_{N2} reported earlier.[10] In stark discrepancy with the value of $M_r = 2.36$ μ_B/f.u. deduced from the NPD, we find that $M_r(T_{N2}) \approx 0.16$ μ_B/f.u., which, on the other hand, is in good agreement with the value given in Ref. 10 for a collection of crystals ($\approx$0.1 μ_B/f.u.). Additionally, in NPD it was found that the Fe_3 and Fe_1 magnetic sublattices give rise to the ferrimagnetic character since they have opposite contributions to the magnetization in the a direction.[8] Therefore, the reduction of M_r indicates that there is a compensation process of the Fe_1 and Fe_3 sublattice magnetization as the temperature decreases below T_{N2}.

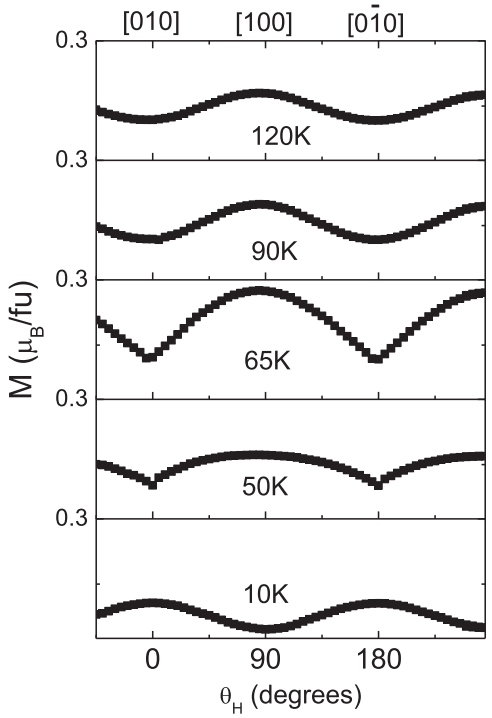

FIG. 7. The projection of the magnetization of $Fe_3O_2BO_3$ in the direction of the applied field upon rotation around the c axis. $H =$ 50 kOe. Note the change of anisotropy EMD at 10 K$<T_{N3}$ to the b axis, while at all other temperatures it is along the a axis.

The high-field slope of the hysteresis curves allows us to determine the subjacent antiferromagnetic susceptibility $\chi_{AFM}(T)$ (see Fig. 8 inset). It has the temperature dependence of an antiferromagnetic system measured along the parallel direction, with ordering temperature at the point of maximum slope below the maximum, which corresponds nicely to the T_{N2} temperature. Since only below this temperature do Fe_1 and Fe_3 sublattice moments become nonzero, as observed by NPD, it can be stated that these sublattices are at the origin

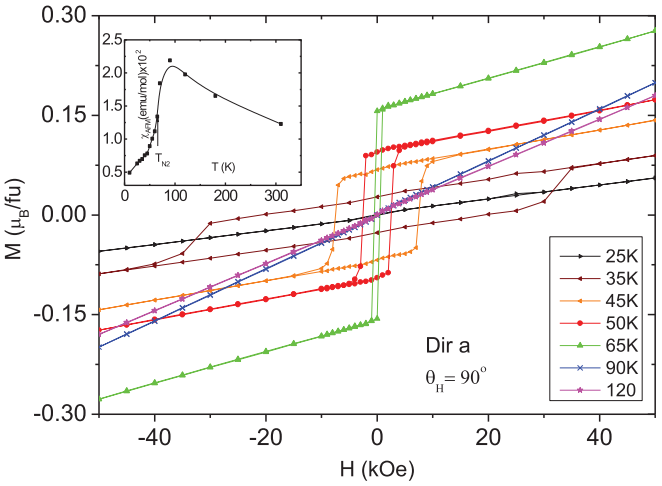

FIG. 8. (Color online) Selected hysteresis cycles of an $Fe_3O_2BO_3$ sample at different temperatures, with H parallel to a axis. Inset: Subjacent antiferromagnetic susceptibility χ_{AFM} in the a direction, determined from the high-field slope of the $M(H)$ cycles.

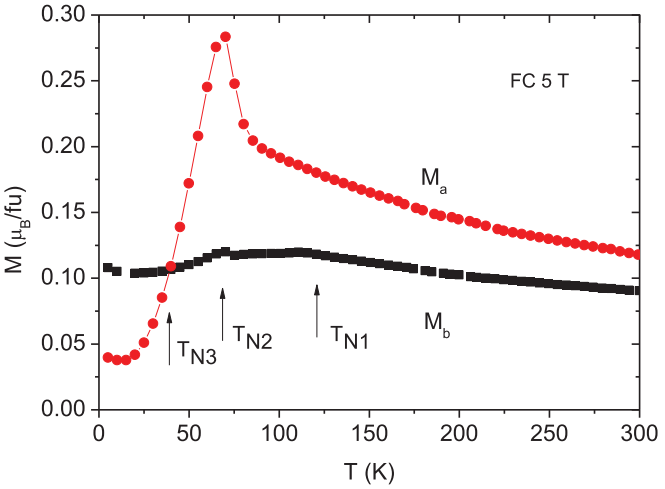

FIG. 9. (Color online) $M_a(T)$ and $M_b(T)$ measurements for $Fe_3O_2BO_3$.

of the AFM subjacent susceptibility along the a axis. This interpretation also agrees with the conclusion reached from MS that Fe_1 and Fe_3 sublattices do not order at T_{N1}, although some polarization from the transferred field of the ordered sublattices is present on Fe_3. Thus, the Fe_1 and Fe_3 sublattices only order below T_{N2}.[14]

$M_a(T)$ and $M_b(T)$, measured at 50 kOe along the a and b axes, respectively, illustrate this compensation behavior clearly (Fig. 9). The transition at T_{N1} gives rise to a change of slope in M_b only, while the transition to the ferromagnetic ordered phase at T_{N2} shows as a peak in both $M_a(T)$ and $M_b(T)$, as could be expected for the establishment of ferrimagnetism.[10] Below T_{N2} there is a decrease in $M_a(T)$ as a consequence of the progressive compensation of the Fe_1 and Fe_3 sublattice magnetization. In fact, at $T \approx 40$ K $M_a(T) = M_b(T)$ and the anisotropy is planar within the ab plane. Below this temperature, b is the EMD of the anisotropic AFM2 phase; i.e., orthogonal to that in the AMF1 or F phase.

C. $Co_{2.25}Fe_{0.75}O_2BO_3$

First, the evidence for the presence and character of the magnetic phase transitions in this compound is obtained from the temperature-dependent susceptibility and magnetization measurements, and later the anisotropy of the single crystal is analyzed by means of the angle-dependent magnetization and hysteresis cycle data.

1. Magnetization temperature dependence

Field-cooled (FC) and zero-field-cooled (ZFC) dc magnetization measurements were performed with applied fields of 100 and 600 Oe on a single crystal. As is seen in Fig. 10 there is a sharp increase of the FC and ZFC magnetization near $T = 70$ K; then the FC value decreases on cooling and the ZFC value drops to zero, being peaklike. Comparing the present data for $Co_{2.25}Fe_{0.75}O_2BO_3$ with the same obtained in Ref. 21 for $Co_2FeO_2BO_3$, one can see that they are very similar. The shape of the magnetization temperature dependence is closer to that of $Fe_3O_2BO_3$, [10] and it is rather different from the same for $Co_3O_2BO_3$.[18,20] There is no sign of the magnetic ordering

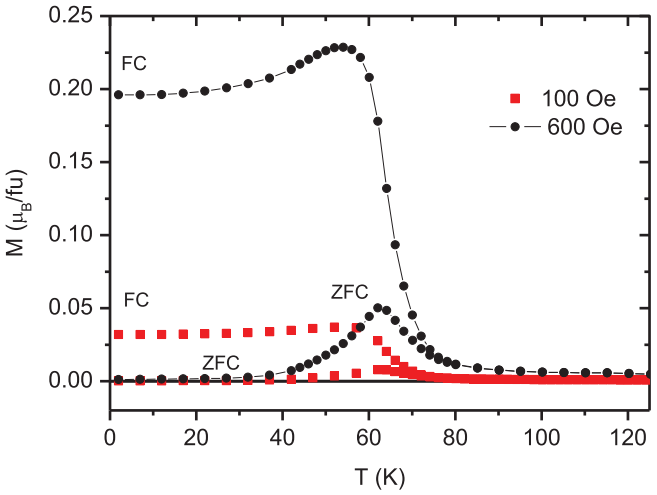

FIG. 10. (Color online) The magnetization temperature dependence of a $Co_{2.25}Fe_{0.75}O_2BO_3$ single crystal.

at 42 K, the characteristic magnetic transition temperature of $Co_3O_2BO_3$, indicating the absence of any spurious fraction of the pure compound in the sample; i.e., the sample is homogeneous.

2. *ac magnetic susceptibility*

The F transition can be clearly observed in the ac magnetic susceptibility temperature dependence at $T_C = 70$ K. For these measurements a single crystal was not large enough to give a good signal-to-noise ratio, so the collective signal for several samples was measured. The temperature behavior of the real χ' and imaginary χ'' components of the magnetic susceptibility is shown in Fig. 11, where a large peak at 70 K and a small anomaly near 115 K are visible. The latter is reminiscent of the AFM1 transition in $Fe_3O_2BO_3$ and corresponds to the beginning of magnetic ordering in our material as seen from the temperature dependence of the MS hyperfine field. The large susceptibility peak is frequency dependent, pointing to domain

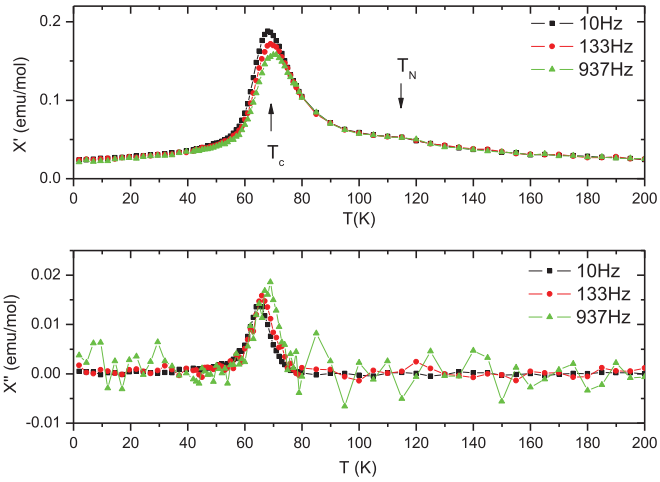

FIG. 11. (Color online) The real and imaginary components of $Co_{2.25}Fe_{0.75}O_2BO_3$ magnetic susceptibility temperature dependences. The arrows indicate the magnetic transitions: a large peak near 70 K and a small anomaly near 115 K.

wall motion of the ferrimagnetic domains. This peak is slightly shifted to higher temperature as the frequency increases.

These ac susceptibility data are also very similar to those for $Co_2FeO_2BO_3$.[21] The analysis of the χ_{dc}^{-1} obtained with the ZFC measurements allows determination of the Curie constant C and the Curie-Weiss temperature θ_C. The results are given in Table I, together with the values for the end members of the row and $Co_2FeO_2BO_3$. For all compounds the θ_C value is negative, pointing out the predominance of antiferromagnetic interactions. The modulus of θ_C increases with Fe content in a regular trend. Consequently, the AFM component of the exchange interaction values is higher for iron ions than for cobalt ions. Our results are on the whole consistent with those previously obtained except for the value of the effective magnetic moment in the paramagnetic phase, which in $Co_{2.25}Fe_{0.75}O_2BO_3$ is closer to that of $Co_3O_2BO_3$ than that of $Co_2FeO_2BO_3$, as shown below. Earlier, the authors of Refs. 20 and 21 defined the effective magnetic moment values averaged for one magnetic ion. In our Table I their results are recalculated as effective magnetic moments per formula unit. As for the effective magnetic moment of $Fe_3O_2BO_3$, defined in Ref. 6, we have calculated a value of $\mu_{\text{eff}} = 9.34\ \mu_B$ per formula unit from their value for the Curie constant $C =$ 10.9 emu K/mol Oe. This value is presented in Table I (row 5) for comparison. All the values calculated by us using the data of Refs. 6,8,20, and 21 are marked by an asterisk.

It is important to estimate the expected values of the effective moment per formula unit in the paramagnetic phase for the considered set of ludwigite compounds to understand whether the orbital moments of magnetic ions are quenched or not. To analyze this question, first, the orbital component of magnetic moment is neglected and the spin component of the effective moment is calculated according to the formula $\mu_s^2 = \sum_i g_i^2 S_i(S_i + 1)$, accounting for the contribution of each type of transition ion. We assumed that all ions are in the high-spin state and that in the mixed ludwigites all iron ions are in the trivalent state. The spin values of the, magnetic ions are Co^{2+}, $S = 3/2$, Co^{3+}, $S = 2$, Fe^{2+}, $S = 2$, and Fe^{3+}, $S = 5/2$; $g = 2$. There are two divalent ions and one trivalent ion in the formula unit. Then, for $Co_3O_2BO_3$ $\mu_S = \sqrt{4[2 \times \frac{3}{2}(\frac{3}{2}+1) + 1 \times 2(2+1)]} =$ 7.35 μ_B. By analogy, for $Co_2FeO_2BO_3$ $\mu_S = \sqrt{4[2 \times \frac{3}{2}(\frac{3}{2}+1) + 1 \times \frac{5}{2}(\frac{5}{2}+1)]} = 8.06\ \mu_B$ and for $Fe_3O_2BO_3$ $\mu_S = \sqrt{4[2 \times 2(2+1) + 1 \times \frac{5}{2}(\frac{5}{2}+1)]} = 9.11\mu_B$. These values are shown in Table I (row 6). Second, we have tried to estimate the expected values of the effective magnetic moment per formula unit, taking into account its orbital component. In this case $\mu_j^2 = \sum_i g_i^2 J_i(J_i + 1)$. The scheme of Co ion electron levels is very sensitive to the crystal field and it is not available at present for all cases of distorted oxygen octahedra in the ludwigite structure. Therefore, we have used the results of Ropka and Radwanski,[23] who have calculated electron level energies and g values for different J for cobalt ions in $LaCoO_3$. According to them, we have assumed for high-spin d^6 ions Co^{3+} and Fe^{2+} $J = 1$, $g = 3.4$. For the high-spin d^7 ion Co^{2+} we assume $J = 1/2$, $g = 2.21$, and for the d^5 ion Fe^{3+} it is clear that $J = S = 5/2$ and $g = 2$. The corresponding values of the effective magnetic moment

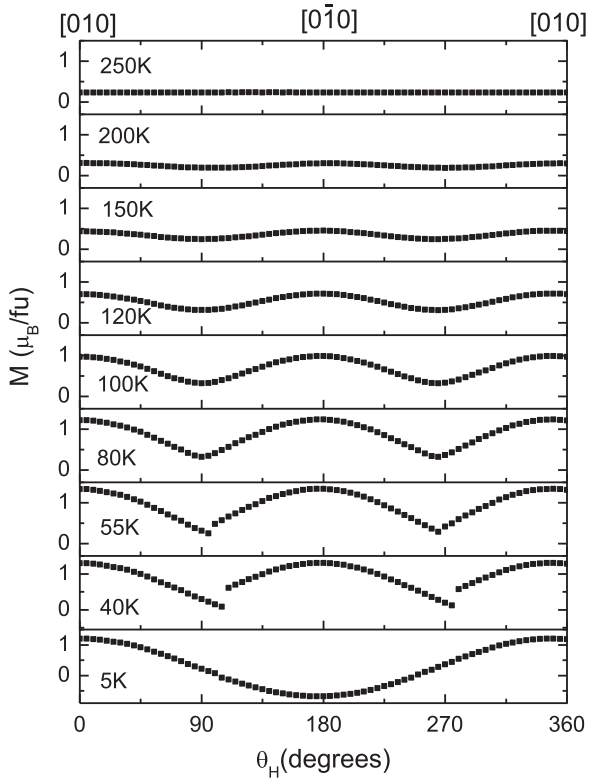

FIG. 12. The projection of the magnetization of $Co_{2.25}Fe_{0.75}O_2BO_3$ in the direction of the applied field upon rotation around the c axis. $H = 50$ kOe.

per formula unit, μ_J, are in Table I (row 7). Comparing the calculated values of μ_S and μ_J with the experimental value μ_{eff}, one can see that the spin value μ_S is closer to it than is μ_J. So we can conclude that the orbital moments of Co and Fe ions are almost quenched.

3. *Magnetic hysteresis*

The main characteristic of $Co_{2.25}Fe_{0.75}O_2BO_3$ is its high anisotropy. Indeed, with the rotating sample holder option which allows us to measure the projection of the magnetization along the field direction it was found that the easy axis of magnetization is b, the [010] axis. This is evidenced in Fig. 12, where we show the projection of the magnetization of $Co_{2.25}Fe_{0.75}O_2BO_3$, $M(\theta_H, T)$ at $H = 50$ kOe, in the direction of the applied field upon rotation around the c axis.

At this field and $T = 5$ K the anisotropy along the b axis is so strong that the magnetization remains oriented along that axis during a 180° revolution, and $M(\theta)$ is fitted with a cosine function superimposed onto a constant antiferromagnetic component. This proves without any ambiguity that the magnetic anisotropy of this crystal is uniaxial along the b axis direction, and implies that at this field and temperature the crystal is saturated in the single-domain state. When the temperature rises, the anisotropy decreases, so that above a certain temperature the applied constant field is capable of inducing a magnetization reversal from the [010] direction to the [0$\bar{1}$0] direction (Fig. 13, 40 K). The reversal of the magnetization is very abrupt, that is, the effect due to the field component perpendicular to the b axis is reversible but

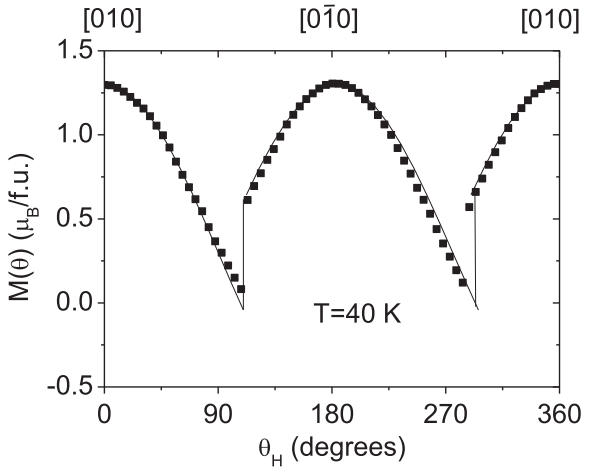

FIG. 13. The projection of the magnetization of $Co_{2.25}Fe_{0.75}O_2BO_3$ in the direction of the applied field upon rotation around the c axis. Note the moment reversion at 110° and return at 288°.

very small, and remains so until the magnetization reversal, while the magnetization reorientation in the b direction is irreversible. Therefore, the field component parallel to the b axis produces the magnetization reversal when $H \cos\theta_H \approx H_C^b$, where H_C^b is the coercive field in the b direction. This behavior is characteristic for systems where the coercive field is much weaker than the anisotropy field. The magnetization reversal cannot occur in unison, but instead by curling or buckling, and the appearance and displacement of domain walls within the sample. It is noteworthy that the anisotropy remains visible above T_C and T_N, up to the paramagnetic phase. The coercive fields at 20, 30, and 40 K could be determined by angular rotation of the applied field (Fig. 13, for $T = 40$ K). We have obtained the following H_c values: 44, 22, and 13 kOe at 20, 30, and 40 K, respectively. As we will see below, these values are similar to the values found from actual hysteresis loops.

$Co_{2.25}Fe_{0.75}O_2BO_3$ is highly anisotropic; therefore the $M(H)$ hysteresis cycles have been measured at several temperatures in the directions parallel to the c axis and perpendicular to it (b axis) on a single crystal (Fig. 14), in the temperature range $70 < T < 115$ K. In the c direction the material behaves as a simple antiferromagnet with a linear magnetization curve at all measured temperatures. Thus the magnetic moments in the compound are fully compensated along the c axis. In contrast, in the b direction the hysteresis cycle below 115 K shows an increase in the magnetization which indicates that already noncompensation of the moments sets in below that temperature. Below T_C the hysteresis cycle is open, thereby showing the existence of ferro- or ferrimagnetic ordering. Both curves tend to the same high-field limit, which indicates that the Co sublattice is already contributing to the magnetization in the region $T_C < T < T_N$, but since the Co sublattice is not yet magnetically ordered it is due to polarization of the Co moments by the Fe ordered sublattice.

The coercive field increases drastically as temperature is lowered (Fig. 15), with a measured maximum $H_C^b = 90$ kOe at 10 K. Below that temperature the coercive field becomes larger than the maximum applied field, 90 kOe, of our setup.

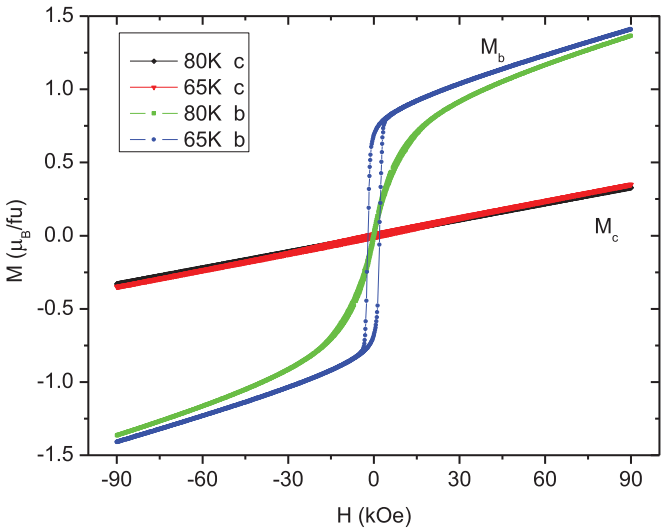

FIG. 14. (Color online) Hysteresis cycles as a function of T ($T \geqslant T_N$). H applied along the b and c axes.

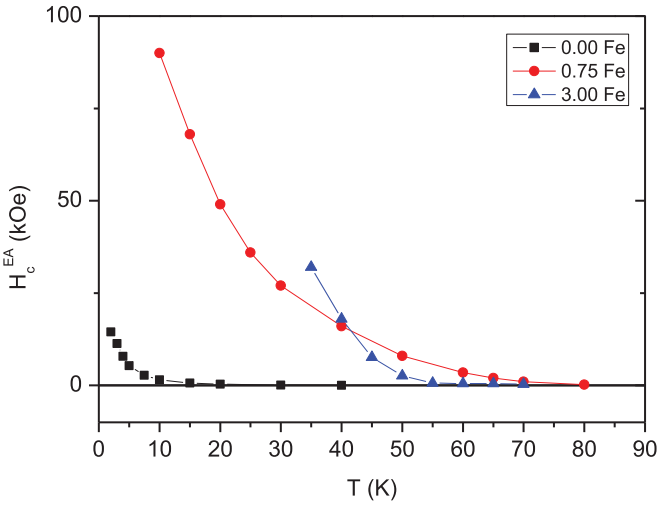

FIG. 16. (Color online) $H_C^b(T)$ for H parallel to the b axis. The data for $Co_{2.25}Fe_{0.75}O_2BO_3$ (●), $Co_3O_2BO_5$ (■), and $Fe_3O_2BO_3$ (▲) are shown.

This is an extraordinarily high coercivity. Superimposed on this fascinating feature is an AFM component, expressed as the absence of saturation and linear dependence of the magnetization on the field at high fields. This behavior is characteristic for an uncompensated antiferromagnet, or a ferrimagnet. Thus, the high-field branches of $M(H)$ are not saturated, but have a positive slope χ_{AFM}. The remanent magnetization M_r and dc susceptibility values χ_{AFM} extracted from hysteresis loops are collected in Table I together with the data obtained earlier for $Fe_3O_2BO_3$, $Co_3O_2BO_3$, and $Co_2FeO_2BO_3$.The maximum values of χ_{AFM} obtained for our sample and those of $Fe_3O_2BO_3$, $Co_3O_2BO_3$, and $Co_2FeO_2BO_3$ are quite close to each other: $\chi_{\mathrm{AFM}} \approx 0.03$ emu/mol. That is, there are several sublattices with AFM coupling but incomplete compensation in this material. It is found that χ_{AFM} is practically isotropic at a fixed temperature. In addition, the remanent magnetization M_r is almost independent of T at low temperatures, and at the coercive field the difference between the magnetization in the up and down orientations is $\Delta M = 2M_r$, which implies that the ferromagnetic component of the magnetization is saturated at a value $M = M_r$.

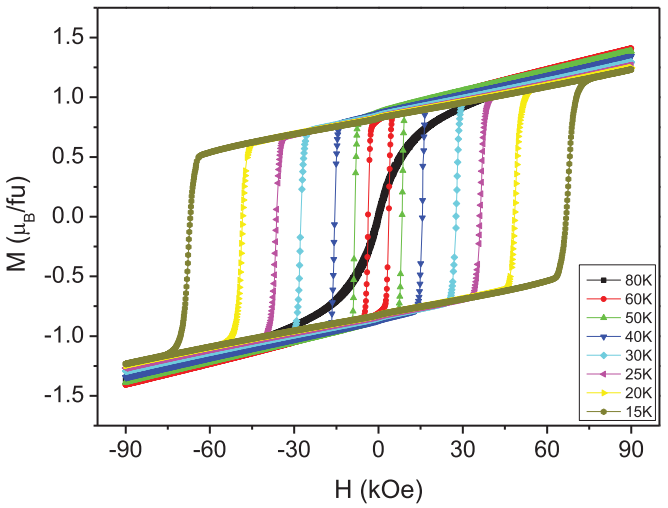

FIG. 15. (Color online) Hysteresis cycles of a $Co_{2.25}Fe_{0.75}O_2BO_3$ sample as a function of T ($T<T_N$). H parallel to the b axis.

In Fig. 16 the $H_C(T)$ curves found for the three samples are compared along their corresponding EMDs. For $Co_3O_2BO_3$, $H_C(T)$ in the b direction increases only below 10 K, while for $Fe_3O_2BO_3$ H_C^a increases rapidly as the temperature decreases once the F phase is reached at T_{N2}, and becomes zero below T_{N3}. It becomes evident that there is a strong increase of $H_C^b(T)$ upon Fe substitution of Co, i.e., at $T = 10$ K the ratio of H_C^b for $Co_{2.25}Fe_{0.75}O_2BO_3$ and $Co_3O_2BO_3$ is about 40.

The similarity of $Co_{2.25}Fe_{0.75}O_2BO_3$ and $Fe_3O_2BO_3$ in magnetic hardness increase with lower temperature explains the similarity in the FC and ZFC $M(T)$ curves of these two compounds, and, in turn, the rather different $M(T)$ in $Co_3O_2BO_3$,[18] which only becomes magnetically hard at much lower temperature.

As can be seen for $Co_{2.25}Fe_{0.75}O_2BO_3$ (Fig. 17, inset), when an external field is applied at an angle θ_H from the b direction, the coercive field increases approximately as $1/\cos\theta_H$ (Kondorsky law).[24] The same dependence is found for $Co_3O_2BO_3$ (Fig. 6, inset). It is justified at low temperatures in view of the fact that the $M(\theta_H)$ curves can be fitted with the expression

$$M(\theta_H) = M_r \cos\theta_H + \chi_{\mathrm{AFM}} H.$$

As mentioned above, the compliance with this $1/\cos\theta_H$ dependence of the angular dependence of the coercive field is characteristic of coercive fields smaller than the anisotropy field. The reason for this behavior may be stress anisotropy or defect pinning of domain walls. Since we are dealing with a single crystal we do not expect stress as the origin of anisotropy but, on the other hand, it is a substitutional system, where many defects in the crystal may be present; therefore, pinned domain walls may account for the coercive field. The coercive field in the b direction due to this mechanism, with 180° domain walls

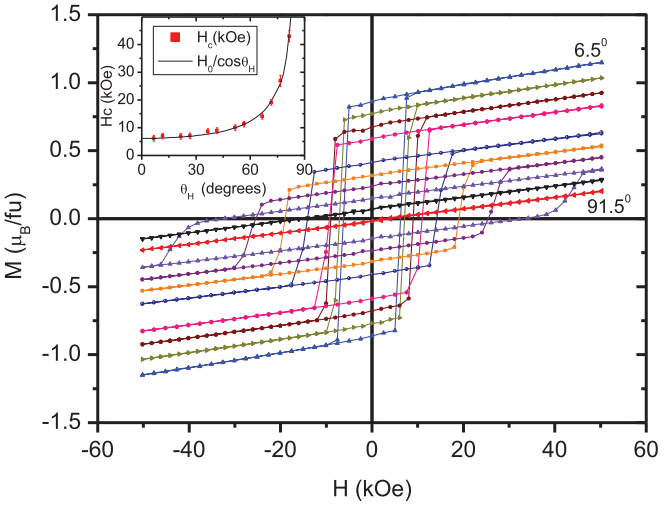

FIG. 17. (Color online) Hysteresis cycles of a $Co_{2.25}Fe_{0.75}O_2BO_3$ single crystal at $T = 50$ K, as a function of rotation around the c axis. The extreme values of θ_H are indicated. The inset shows the variation of H_C as a function of θ_H. The fit to a $1/\cos\theta_H$ function is also shown.

being created and propagated at the switching field gives a coercive field

$$H_C^b(\theta_H) = \frac{\gamma}{\cos\theta_H l M_r},$$

where γ is the domain wall energy and l is the average defect-defect distance. The temperature dependence of this coercive field enters via the dependence of the wall energy on the anisotropy constant K_1, $\gamma \propto \sqrt{AK_1}$, where A is proportional to the exchange coupling.[25] For comparison, at the same temperature $T = 10$ K, and $\theta_H = 0$ one obtains $H_C^b M_r = \gamma/l = 8.73\times10^6$ and 7.46×10^5 G^2 for $Co_{2.25}Fe_{0.75}O_2BO_3$ and $Co_3O_2BO_3$, respectively, i.e., an order of magnitude increase upon the Co substitution by Fe. Since T_C is larger and therefore A is larger for $Co_{2.25}Fe_{0.75}O_2BO_3$, but not enough to explain the observed increase, and K_1 may be similar in both compounds, it can be concluded that the main reason for the increase in coercivity field is the increase of the number of defects in the crystal upon the introduction of Fe, which in turn reduces strongly the average distance between defects, l.

The comparison of M_r of $Co_{2.25}Fe_{0.75}O_2BO_3$ with that of $Co_3O_2BO_3$ may now be done with the present measurements of the hysteresis cycles of the single crystal of the latter compound, since in Ref. 18 it could not be discerned whether the M_r data corresponded to a single crystal or a collection of crystals with different orientations. The value found is $M_r = 3.4(1)$ μ_B/f.u., i.e., much larger than the previously published result, most probably because of the fact that our measurement was on an oriented single crystal. Additionally, in the present work the remanent magnetization in the $Fe_3O_2BO_3$ a direction was found in the F phase to be $M_r(T = 65\ \text{K}) = 0.16$ μ_B/f.u., similar to the average value previously published of 0.1 μ_B at 70 K,[10] and drastically different from the powder neutron diffraction value[8] 2.36 μ_B/f.u. On the other hand, the value given for $Co_2FeO_2BO_3$ (0.48 μ_B/f.u.) is half that found for $Co_{2.25}Fe_{0.75}O_2BO_3$ (0.9 μ_B/f.u.), although we explain this difference in the former compound as due to possible misorientation of the crystal in that paper. From this comparison a very puzzling conclusion is drawn. The effect of substitution of 25% of Co atoms by Fe is a dramatic decrease of M_r, which cannot be explained by the Co moments ($\mu_{\text{eff}} = 7.2$ μ_B) being substituted by Fe moments ($\mu_{\text{eff}} = 8.01$ μ_B).

One striking result of this work is the drastic reduction of magnetic moment in the b direction with respect to the $Co_3O_2BO_3$ compound. A naive accounting of the magnetic moment per Co in $Co_3O_2BO_3$ yields $m_{\text{Co atom}} = M_r/3 = 1.15$ μ_B/Co along the b direction; therefore in $Co_{2.25}Fe_{0.75}O_2BO_3$ the Co sublattice should account for $m_{\text{Co sublattice}} = 2.58$ μ_B, while the observed $M_r = 0.9$ μ_B. The difference can be conjectured to be caused by the Fe moments being oriented with a component of the Fe sublattice $m_{\text{Fe}} = -1.68$ μ_B ($|m_{\text{Fe atom}}| = 2.24$ μ_B/Fe); i.e., opposing the net moment of the Co sublattice. Indeed, if the Fe moments order similarly as in $Fe_3O_2BO_3$, the moments at sites 2 and 4 will be oriented in the b direction and will tend to compensate one another, and will also oppose the Co magnetic moment in that direction. There should be an interplay of compensation of Co moments in the diluted compound and probably Fe-Co antiferromagnetic interactions to account for the reduction of M_r.

In Ref. 22 a simplified model of Fe substitution is proposed to study the effect of Fe-Co interactions, where only position 4 is assumed to be occupied by Fe. The superexchange interactions between Co-Co and Co-Fe ions are estimated, and the conclusion reached is that the Co_3-Fe_4 exchange interaction tends to orient the Fe_4 magnetic moment in the opposite direction from that of the Co_4 moment it has substituted. Although other interactions may be present, this gives us a clue as to the reason for the strong reduction in magnetic moment that we have observed in the b direction.

Another possibility is that Co^{3+} transforms from high-spin to intermediate- or low-spin states upon reduction of cell volume when Co is substituted by Fe. Obviously, the magnetic structure of $Co_3O_2BO_3$ is not yet known; therefore it is not possible to go further into the analysis of this puzzling result.

V. DISCUSSION AND CONCLUSIONS

The x-ray data obtained in the present work have shown that there are some difficulties in the synthesis of the solid solution $Co_{3-x}Fe_xO_2BO_3$ oxyborates with the ludwigite structure with high iron content. When the x value exceeds 1 the material tends to crystallize in the warwickite structure. The unit cell volume of the mixed ludwigites exceeds the values expected from Vegard's law.

This work provides information on single crystals that clarifies the magnetic properties of the pure compounds along their crystallographic axes. In $Co_3O_2BO_3$ it has been established that the b axis is the EMD in the ferromagnetic phase and the dependence of H_c with temperature has been found.

In $Fe_3O_2BO_3$ the a axis is the EMD down to T_{N3}, below which it is the b axis. The Fe_2 and Fe_4 sublattices order antiferromagnetically at T_{N1}, and the Fe_1 and Fe_3 sublattices order as a ferrimagnet at T_{N2} with their moments parallel to the a direction. The subjacent antiferromagnetic ordering of these sublattices, once the ferrimagnetism is saturated by the

field, is clearly seen to set in at that temperature (Fig. 8 inset). The AFM2 phase is reached continuously at approximately T_{N3}, as the temperature decreases from the F phase, by compensation of the Fe_1 and Fe_3 oppositely oriented sublattice magnetizations.

In the solid solution $Co_{2.25}Fe_{0.75}O_2BO_3$ the paramagnetic effective magnetic moment per formula unit at high temperatures is slightly higher than for $Co_3O_2BO_3$, as expected. The spin-only values of the effective magnetic moments in Co-Fe ludwigites appear to be closer to the experimental values than the total one, calculated using J and g values obtained in Ref. 23. This indicates that the orbital moment of magnetic ions in these compounds is quenched to a high degree.

The hyperfine field splitting of the quadrupole doublets into sextets (Fig. 2) and a small anomaly in the magnetic susceptibility near $T_N = 115$ K (Fig. 11) have been observed, which hint at an antiferromagnetic transition of the 3LL type-I sublattice. Indeed, in Ref. 8, devoted to $Fe_3O_2BO_3$ it was shown that at this temperature the 3LL type-I sublattice orders while the 3LL type-II sublattice remains without long-range magnetic ordering. The definite clue for the long-range ordering of the 3LL type-I sublattice was the detection of a peak at T_N in the heat capacity of $Fe_3O_2BO_3$. Such a peak was also detected in $Co_2FeO_2BO_3$,[21] which has the same ac susceptibility bump near 110 K as we have observed in $Co_{2.25}Fe_{0.75}O_2BO_3$. Moreover, in Fig. 14 it is demonstrated that there is a magnetic moment developing in the b direction at 80 K, albeit the compound is not yet magnetically ordered. We conclude that the transition from the PM to the AFM1 phase takes place already at a dilution fraction of Co:Fe of 3:1. So, in $Co_{2.25}Fe_{0.75}O_2BO_3$ we deal with partial magnetic ordering as in $Fe_3O_2BO_3$ in the intermediate region $T_C < T < T_N$, in contrast to absence of this intermediate phase in $Co_3O_2BO_3$.

The large susceptibility peak at $T_C = 70$ K and the open hysteresis cycles below this temperature show that $Co_{2.25}Fe_{0.75}O_2BO_3$ orders ferrimagnetically. The frequency dependence of this susceptibility peak may be explained as due to the magnetic domain motion of the ferromagnetic domains. Ferrimagnetism rather than weak ferromagnetism is preferable to describe this transition since the net moment originates from magnetic moments of different modulus and orientation, rather than from identical moments with near but not complete antiferromagnetic compensation by orientation; however, there is some ambiguity in naming this transition in the literature. The same type of transition is described in $Fe_3O_2BO_3$ in Ref. 10; its authors propose that this peak shows additional ordering of the ions in the positions 1. More recently, in Ref. 8 it is shown by neutron diffraction that the Fe moments at positions 1 and 3 develop each a different net moment, oppositely oriented, giving rise to a ferrimagnetic ordering. So, on one hand, by similarity with $Fe_3O_2BO_3$, one would expect the few Fe moments entering into sites 1 in the 3LL type-II sublattice to contribute to the net moment in the a direction; however, we observe no net moment in this direction. On the other hand, the compensation of Co and Fe moments in the 3LL type-I sublattice should give a second contribution to the ferromagnetic moment below T_C. The net effect observed is a strong reduction in the ferromagnetic moment in the b direction and compensated antiferromagnetism in the c direction. In our opinion the frequency dependence of ac susceptibility peak near 70 K in the mixed ludwigites originates rather from the motion of ferrimagnetic domain walls than from partial spin-glass freezing.

It is surprising that in our magnetic data there is no sign of a magnetic phase transition at 42 K, the T_N of $Co_3O_2BO_3$. Our magnetic results are very similar to those obtained in Ref. 21 for $Co_2FeO_2BO_3$. In that paper, partial magnetic ordering of some of the magnetic ions near 117 K and a spin-glass freezing of the remainder near 70 K is proposed.

The magnetic ordering of $Co_{2.25}Fe_{0.75}O_2BO_3$ below T_N has a predominant ferromagnetic moment on the b axis, just as in $Co_3O_2BO_3$, and antiferromagnetic components in all directions, the contribution being nearly isotropic. The ground state seems to be ferrimagnetic. The remanent magnetization of $Co_{2,25}Fe_{0,75}O_2BO_3$ is much lower compared to $Co_3O_2BO_3$, but the coercive field is much higher. The $1/\cos\theta_H$ law followed by the coercive field angle dependence indicates that we are dealing with the case of a very large crystalline anisotropy field, larger than the coercive field. H_C depends essentially on the number of defects in the crystal, while the temperature dependence of H_C is driven by the increase of the anisotropy constant K_1 with decreasing temperature.

The anisotropy in the b direction is the same as that in $Co_3O_2BO_3$ and different from that in the ferrimagnetic phase of $Fe_3O_2BO_3$, where the EMD is the a axis, according to the present work and neutron diffraction results.[8] For this reason, it is impossible at this stage to conjecture what is the orientation of the Fe inserted moments, except that they compensate strongly the net moment of the Co sublattice, giving rise to a strong decrease of M_r. It has been proposed from a simplified model that the Fe_4-Co_3 superexchange interaction tends to orient the Fe moment in the opposite direction to that of the Co_4 it has substituted,[22] thus explaining partially the strong reduction in M_r observed.

Obviously, neutron diffraction experiments on $Co_3O_2BO_3$, as reference, and on $Co_{2.25}Fe_{0.75}O_2BO_3$ are needed to clarify this question. An open question is the fact that the anisotropy is very high while, as argued in Sec. IV, the orbital moment is highly quenched. The origin of the anisotropy, therefore, has to be related to exchange interactions between the Co and Fe moments.

The magnetic behavior of $Co_{2.25}Fe_{0.75}O_2BO_3$ may also be compared to that of the heterometallic ludwigites with different transition metals Ni and Cu. These compounds undergo three successive magnetic phase transitions at $T_{N1} > T_{N2} > T_{N3}$. In $Ni_2FeO_2BO_3$, $T_{N1} = 106$ K, $T_{N2} = 46$ K, and $T_{N3} = 14$ K,[2] while in $Cu_2FeO_2BO_3$, $T_{N1} = 63$ K, $T_{N2} = 38$ K, and $T_{N3} = 20$ K.[3] They are explained in terms of a hierarchy of interactions such that at T_{N1} only the Fe sublattice orders partially, at T_{N2} the transition metal sublattice orders independently, and only at T_{N3} do the two sublattices couple and give rise to the reentrant AFM2 phase. It may be concluded that in the three cases the substitution of the transition metal by Fe induces the ordering of the Fe sublattice at T_{N1} (T_N in our case), an indication of the strong Fe-Fe interaction. However, in $Co_{2.25}Fe_{0.75}O_2BO_3$ we have shown in Fig. 14 that below T_{N1} the Co sublattice already gives an important contribution to the magnetization in the b direction, probably through polarization

by the Fe sublattice; therefore the Fe-Co coupling is already effective below T_{N1}. In addition, the phase below T_{N2} (T_C in the Co case) is ferromagnetic in the Co compound, while in the Ni and Cu cases it is antiferromagnetic, on one hand, and does not undergo any reentrant transition, on the other. It can be concluded that the Fe-Co coupling is stronger than that for Ni or Cu, probably due to the lower magnetic moment of these atoms with respect to Co.

In this work we showed unambiguously that Fe substitution induces an extraordinarily high uniaxial anisotropy along the [010] axis in the $Co_3O_2BO_3$ compound, and a strong decrease in the net ferromagnetic moment. For further understanding of the competing roles of Fe and Co in this structure, the magnetic structure determination of $Co_3O_2BO_3$ with neutron diffraction would be of paramount importance.

ACKNOWLEDGMENTS

The authors acknowledge V. V. Rudenko for the oxyborate samples they made and O. A. Bayukov for fruitful discussion. The financial support of Spanish MINCYT, Grant No. MAT08/1077, and the Aragonese E-34 project are acknowledged. Fruitful discussions with F. Bartolomé and P. Bordet are acknowledged. The latter is thanked for providing the $Fe_3O_2BO_3$ single crystal. Also this study was supported by the Russian Foundation for Basic Research (Project No. 09-02-00171-a), the Federal Agency for Science and Innovation (Rosnauka) (Project No. MK-5632.2010.2), and the Physical Division of the Russian Academy of Science (Program "Strongly Correlated Electrons," Project No. 2.3.1).

[1] R. Norrestam, M. Kritikos, K. Nielsen, I. Sotofte, and N. Thorup, J. Solid State Chem. **111**, 217 (1994).
[2] J. C. Fernandes, R. B. Guimaraes, M. A. Continentino, H. A. Borges, A. Sulpice, J-L. Tholence, J. L. Siqueira, L. I. Zawislak, J. B. M. da Cunha, and C. A. dos Santos, Phys. Rev. B **58**, 287 (1998).
[3] M. A. Continentino, J. C. Fernandes, R. B. Guimaraes, H. A. Borges, A. Sulpice, J-L. Tholence, J. L. Siqueira, J. B. M. da Cunha, and C. A. dos Santos, Eur. Phys. J. B **9**, 613 (1999).
[4] J. C. Fernandes, R. B. Guimaraes, M. Mir, M. A. Continentino, H. A. Borges, G. Cernichiaro, M. B. Fontes, and E. M. Baggio-Saitovich. Physica B **281/282**, 694 (2000).
[5] J. S. Swinnea and H. Steinfink, Am. Mineral. **68**, 827 (1983).
[6] M. Mir, R. B. Guimaraes, J. C. Fernandes, M. A. Continentino, A. C. Doriguetto, Y. P. Mascarenhas, J. Ellena, E. E. Castellano, R. S. Freitas, and L. Ghivelder, Phys. Rev. Lett. **87**, 147201 (2001).
[7] A. Latge and M. A. Continentino, Phys. Rev. B **66**, 094113 (2002).
[8] P. Bordet and E. Suard. Phys. Rev. B **79**, 144408 (2009).
[9] J. P. Attfield, J. F. Clarke, and D. A. Perkins, Physica B **180**, 581 (1992).
[10] R. B. Guimaraes, M. Mir, J. C. Fernandes, M. A. Continentino, H. A. Borges, G. Cernicchiaro, M. B. Fontes, D. R. S. Candela, and E. Baggio-Saitovitch, Phys. Rev. B **60**, 6617 (1999).
[11] J. A. Larrea, D. R. Sanchez, F. J. Litterst, and E. M. Baggio-Saitivich, J. Phys.: Condens. Matter **13**, L949 (2001).
[12] J. A. Larrea, D. R. Sánchez, E. M. Baggio-Saitovich, J. C. Fernandes, R. B. Guimaraes, M. A. Continentino, and F. J. Litterst, J. Magn. Magn. Mater. **226**, 1079 (2001).
[13] A. P. Douvalis, A. Moukarika, T. Bakas, G. Kallias, and V. Papaefthymiou, J. Phys.: Condens. Matter **14**, 3303 (2002).
[14] J. Larrea, D. R. Sanchez, F. J. Litterst, E. M. Baggio-Saitovitch, J. C. Fernandes, R. B. Guimaraes, and M. A. Continentino, Phys. Rev. B **70** 174452 (2004).
[15] J. Dumas, J. L. Thompson, M. Contentino, J. C. Fernandes, R. B. Guimaraes, and M. H. Whangbo, J. Phys. IV **12**, Pr9-351 (2002).
[16] E. Vallejo and M. Avignon, Phys. Rev. Lett. **97**, 217203 (2006).
[17] Z.-X. Huang, W.-D. Cheng, and H. Zhang, Chin. J. Struct. Chem. **20**, 97 (2001).
[18] N. B. Ivanova, A. D. Vasil'ev, D. A. Velikanov, N. V. Kazak, S. G. Ovchinnikov, G. A. Petrakovskii, and V. V. Rudenko, Phys. Solid State **49**, 651 (2007).
[19] N. V. Kazak, N. B. Ivanova, V. V. Rudenko, A. D. Vasil'ev, D. A. Velikanov, S. G. Ovchinnikov, and Yu. V. Knyazev, Phys. Solid State **51**, 966 (2009).
[20] D. C. Freitas, M. A. Continentino, R. B. Guimaraes, J. C. Fernandes, J. Ellena, and L. Ghivelder, Phys. Rev. B **77**, 184422 (2008).
[21] D. C. Freitas, M. A. Continentino, R. B. Guimaraes, J. C. Fernandes, E. P. Oliveira, R. E. Santelli, J. Ellena, G. G. Elsava, and L. Ghivelder, Phys. Rev. B **79**, 134437 (2009).
[22] N. V. Kazak, N. B. Ivanova, O. A. Bayukov, S. G. Ovchinnikov, A. D. Vasiliev, V. V. Rudenko, J. Bartolomé, A. Arauzo, and Yu. V. Knyazev, J. Magn. Magn. Mater. **323**, 521 (2011).
[23] Z. Ropka and R. J. Radwanski, Phys. Rev. B **67**, 172401 (2003).
[24] E. Kondorsky, Phys. Z. Sowjetunion **11**, 597 (1937).
[25] S. Chikazumi, *Physics of Magnetism* (John Wiley & Sons, New York, 1964).